Analytical Approach for Evaluation of Lithium-Ion Battery Cells

Sebastian Wagner,*[a, b] Alexander Oberland,[b, c] and Thomas Turek[a, b]

A new method for evaluation of battery cells containing porous thin-layer electrodes is developed. For this purpose, a typical concept of chemical reaction engineering to classify reactors by dimensionless characteristic values is used. Therefore, the system of equations describing the porous electrodes in a battery cell is transferred to dimensionless notation and corresponding dimensionless properties are developed. The required kinetic data are measured with the help of electrochemical test cells. A complete set of parameters for the description of the lithium-ion battery is determined and the characteristic properties for the chosen example are calculated and analyzed. Finally, the performance of the anode and cathode using lithium manganese oxide and surface-modified graphite as active materials is compared with the aid of the newly developed dimensionless parameters.

Introduction

The widespread use of lithium-ion batteries (LIBs) in stationary and portable applications as well as in electromobility requires criteria for classification and evaluation of electrodes and full battery cells. LIB cells are electrochemical reactors transforming chemical energy into electric power reversibly, so characteristic values can be formulated for this purpose. LIB technology has been established already in 1976.[1,2] Modern LIB research is focused on the development of improved active materials[3,4] as well as on engineering issues.[5] Especially the design optimization of LIB is a major challenge and has been investigated by extensive parameter studies[6,7] for different numbers of variables[8,9] on various model scales.[10] Some of these parameter studies are complex, typically requiring a high computational effort. The new method should provide a reasonable and time-saving alternative.

Properties such as capacity, energy, or power density are describing the competitiveness of active materials and full battery cells. Nevertheless, the performance of an electrode is influenced by many factors. Therefore, it is suggested to transfer the concept of chemical reaction engineering for evaluating reactors with dimensionless characteristic values to battery technology. The informative value of single parameters is often low because of their simultaneous impact on several of the mentioned cell characteristics. Therefore, an abstraction of the considered system is necessary to separate and analyze different properties for limiting factors in fundamental processes. During this abstraction dimensionless properties are defined, for example, for single electrodes, and their values are compared and evaluated. A full set of characteristic values will be established in this way. For this purpose, a simple basic battery model is used, which will be transferred to dimensionless notation. This basic model could be extended in subsequent work to incorporate further effects of interest in the characteristic values or to define new quantities. As a first application of the analytical approach, the impact of a single characteristic value will be elaborated.

Dimensionless modeling of single particles[11] and full battery cells[12,13] as well as dimensional analysis[14] have already been applied to LIB cells. Newman et al.[12,15] defined the ratio of discharge time and diffusion time both for electrode and particle at an early stage of LIB modeling whereas Du et al.[14] extended this theory to a dimensionless material conductivity. Zhang et al.[11] contributed the ratio of diffusion resistance to reaction resistance for single particles. However, there are further quantities with impact on the performance of battery cells such as the dimensionless electrolyte conductivity. Thus, consistent application of dimensionless quantities to battery modeling is still required.

For the first application of a complete set of dimensionless characteristic values, a LIB standard cell shown in Figure 1 is specified and simulated. Active materials used in the stan-

[a] S. Wagner, Prof. Dr. T. Turek
Institute of Chemical and Electrochemical Process Engineering
Clausthal University of Technology
Leibnizstraße 17, 38678 Clausthal-Zellerfeld (Germany)
E-mail: wagner@icvt.tu-clausthal.de

[b] S. Wagner, A. Oberland, Prof. Dr. T. Turek
Energie-Forschungszentrum Niedersachsen (EFZN)
Am Stollen 19A, 38640 Goslar (Germany)

[c] A. Oberland
Institute of Electrical Power Engineering and Energy Systems
Clausthal University of Technology
Leibnizstraße 28, 38678 Clausthal-Zellerfeld (Germany)

Part of a Special Issue on "Li-Ion Batteries". To view the complete issue, visit: http://dx.doi.org/10.1002/ente.v4.12

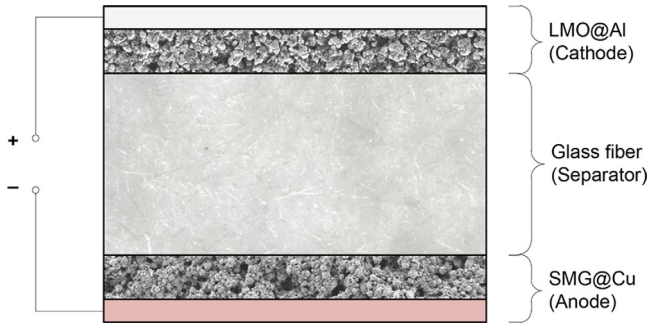

Figure 1. LIB standard cell.

dard cell are lithium manganese oxide (LMO) and surface-modified graphite (SMG). The reversible lithium intercalation reactions can be described by Equations (1) and (2).

$$LiMn_2O_4 \rightleftharpoons Li_{1-x}Mn_2O_4 + x\,Li^+ + x\,e^- \quad (1)$$

$$n\,C + x\,Li^+ + x\,e^- \rightleftharpoons Li_xC_n \quad (2)$$

Results and Discussion

Measured data

The complete set of parameters for experimental investigations and simulation of the LIB standard cell is summarized in Table 1.

The specific surface area related to the electrode layer volume can be calculated from the average particle radius [Eq. (3)].

$$a_v = \frac{3}{R_1} \cdot \varepsilon_1 \quad (3)$$

The definitions of the variables can be found in Table 6. The maximum lithium concentration of the active material was determined by measuring the capacity of the electrodes (approximately 3.3 mAh in both cases) in half cells using the following relationship [Eq. (4)]

$$q = z \cdot F \cdot \varepsilon_1 \cdot \delta \cdot c_s \quad (4)$$

whereas the state of charge (SoC) is defined by Equation (5):

$$SoC = \frac{q}{q_{max}} = \frac{c_s}{c_{s,max}} \quad (5)$$

Kinetic parameters were determined using the linear polarization method. The measurements were carried out in a climate chamber at 20 °C. Transfer coefficients and the exchange current were estimated with the aid of the Tafel fit analysis tool from EC-Lab® for several states of charge. This fitting tool utilizes the Tafel approximation at increased overpotentials (anodic: >25 mV, cathodic: >15 mV). The obtained transfer coefficients were normalized to one whereas the determined exchange currents were converted into exchange rates with Faraday's law. Reaction rate constants were adjusted to measured data using linear regression, the corresponding exchange rates are shown in Figure 2.

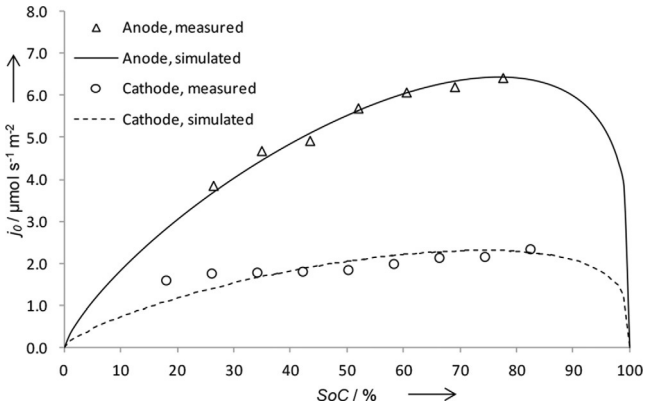

Figure 2. Calculated and measured exchange rates as a function of SoC for anode and cathode at 20 °C.

The measured data during the charging process of the LIB test cell are compared with simulation results in Figure 3. For this purpose, the set of parameters in Table 1 and the set of equations in Table 2 were used.

Table 1. Set of parameters for LIB test cell.

Parameter	Anode	Separator	Cathode	Unit
A	254.5	254.5	254.5	mm^2
δ	48.2	1450	58.8	µm
ε	64.8	91.7	39.0	%
ε_1	31.0		48.9	%
R_1	7.04		4.55	µm
σ	75 [a]		3 [a]	S m^{-1}
D_s	$5\cdot10^{-14}$ [a]		$5\cdot10^{-14}$ [a]	m^2 s^{-1}
D_{Li}		$3.47\cdot10^{-10}$ [b]		m^2 s^{-1}
t^0_{Li}		0.28 [b]		–
$c_{Li,0}$		1		mol dm^{-3}
$c_{s,max}$	32.36		16.84	mol dm^{-3}
α_{ox}	0.23		0.26	–
α_{red}	0.77		0.74	–
k	$6.94\cdot10^{-11}$		$4.06\cdot10^{-11}$	mol^{1-X} m$^{3\cdot X-2}$ s^{-1}
T		293.15		K

[a] Estimated value. [b] Ref. [16].

Model setup

Appropriate models for simulation of rechargeable batteries are well known[17] and have been also published for LIBs.[15,18] A reduced system of differential equations and kinetics summarized in Table 2 was implemented and solved in MATLAB® using the finite volume method (FVM).

Operational parameters are the current density i that splits into ionic (i_1) and electric (i_2) fractions inside porous electrodes

$$i = i_1 + i_2 \quad (6)$$

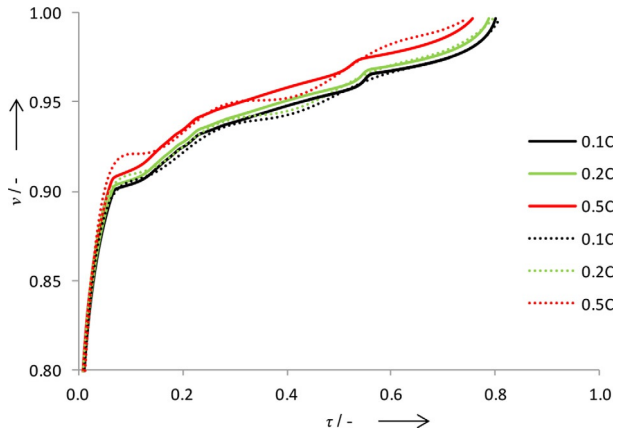

Figure 3. Dimensionless cell voltage of the LIB test cell as a function of dimensionless charging time (solid lines: measured data; dashed lines: simulation results).

and the cell voltage U, which results from the solid phase potential at both current collectors.

$$U = \Phi_1(x_c = \delta_c) - \Phi_1(x_a = 0) \tag{7}$$

Voltage losses in the current collectors, made of aluminum and copper, can be neglected in case of non-wound test cells with small electrode area. In the following, the described set of model equations was transferred to dimensionless formulations. Definitions of the dimensionless variables used are listed in Table 3.

Table 3. Definition of dimensionless variables.

Variable	Definition
lithium ion concentration	$f_{Li} = \frac{c_{\mathrm{Li}}}{c_{\mathrm{Li},0}}$
lithium concentration	$f_{s,j} = \frac{c_{s,j}}{c_{s,\max,j}} = \frac{q_j}{q_{\max,j}}$
time	$\tau = \frac{t}{t^{\mathrm{ref}}}$
spatial coordinate	$\xi_j = \frac{x_j}{\delta_j}$
radial coordinate	$\lambda_j = \frac{r_j}{R_{1,j}}$
transference number	$t^0_{\mathrm{Li}} = \frac{i_{\mathrm{Li}}}{i_2}$
current density	$\mu_1 = \frac{i_1}{i}, \ \mu_2 = \frac{i_2}{i}$
potential	$\varphi_1 = \frac{\Phi_1}{U^{\mathrm{ref}}} \ \ \varphi_2 = \frac{\Phi_2}{U^{\mathrm{ref}}}$
cell voltage	$\nu = \frac{U}{U^{\mathrm{ref}}}$
reaction rate	$\rho_j = \frac{j_{p,j}}{j^{\mathrm{ref}}_{0,j}}$

Mass transport

The dimensionless material balance for the lithium ions in the electrolyte reads

$$\frac{\partial f_{\mathrm{Li}}}{\partial \tau} = A_{1,j} \cdot \frac{\partial^2 f_{\mathrm{Li}}}{\partial \xi_j^2} - A_{2,j} \cdot \mu_2 \cdot \frac{\partial t^0_{\mathrm{Li}}}{\partial \xi_j} + A_{3,j} \cdot \left(1 - t^0_{\mathrm{Li}}\right) \cdot \rho_j \tag{8}$$

with the dimensionless coefficients A_1, A_2, and A_3. For constant transference numbers, the second term on the right hand side, which represents migration transport, can be neglected. The corresponding balance for the lithium in the active materials yields

$$\frac{\partial f_{s,j}}{\partial \tau} = A_{4,j} \cdot \frac{1}{\lambda_j^2} \cdot \frac{\partial}{\partial \lambda_j}\left(\lambda_j^2 \cdot \frac{\partial f_{s,j}}{\partial \lambda_j}\right) \tag{9}$$

with the dimensionless coefficient A_4.

Charge transfer

The charge balance for the electrodes in dimensionless form is given by Equation (10):

Table 2. Set of equations for LIB simulation.

Description	Equation	
material balance (electrolyte)	$\varepsilon_j \cdot \frac{\partial c_{\mathrm{Li}}}{\partial t} = \frac{\partial}{\partial x_j}\left(D_{\mathrm{Li,eff}} \cdot \varepsilon_j \cdot \frac{\partial c_{Li}}{\partial x_j}\right) - \frac{i_2}{z \cdot F} \cdot \frac{\partial t^0_{\mathrm{Li}}}{\partial x_j} + \left(1 - t^0_{\mathrm{Li}}\right) \cdot a_{v,j} \cdot j_{p,j}$	
material balance (particle)	$\frac{\partial c_{s,j}}{\partial t} = \frac{1}{r_j^2} \cdot \frac{\partial}{\partial r_j}\left(D_{s,j} \cdot \frac{1}{r_j^2} \cdot \frac{\partial c_{s,j}}{\partial r_j}\right)$	
charge balance	$\frac{\partial i_2}{\partial x_j} = z \cdot F \cdot a_{v,j} \cdot j_{p,j}$	$\frac{\partial i_1}{\partial x_j} + \frac{\partial i_2}{\partial x_j} = 0$
Ohm's law	$\frac{\partial \Phi_1}{\partial x_j} = -\frac{i_1}{\sigma_{\mathrm{eff},j}}$	$\frac{\partial \Phi_2}{\partial x_j} = -\frac{i_2}{\kappa_{\mathrm{eff}}}$
kinetics	$j_{p,j} = j_{0,j} \cdot \left[\exp\left(b_{\mathrm{ox},j} \cdot \eta_j\right) - \exp\left(-b_{\mathrm{red},j} \cdot \eta_j\right)\right]$ $j_{0,j} = k_j \cdot c_{Li}^{\alpha_{\mathrm{ox},j}} \cdot \left(c_{s,\max,j} - c_{s,j}\right)^{\alpha_{ox,j}} \cdot c_{s,j}^{\alpha_{\mathrm{red},j}}$	$b_j = \alpha_j \cdot \frac{z \cdot F}{R \cdot T}$ $\eta_j = \Phi_1 - \Phi_2 - U_{0,j}$

$$\frac{\partial \mu_2}{\partial \xi_j} = A_{5,j} \cdot \rho_j \tag{10}$$

where A_5 is a further dimensionless coefficient. Charge conservation leads to the relationship described by Equation (11).

$$\frac{\partial \mu_1}{\partial \xi_j} + \frac{\partial \mu_2}{\partial \xi_j} = 0 \tag{11}$$

Potential drop

The transformation of Ohm's law in the solid phase

$$\frac{\partial \varphi_1}{\partial \xi_j} = -A_{6,j} \cdot \mu_1 \tag{12}$$

and in the liquid phase

$$\frac{\partial \varphi_2}{\partial \xi_j} = -A_{7,j} \cdot \mu_2 \tag{13}$$

results in the dimensionless coefficients A_6 and A_7. In case of the liquid phase potential, the influence of the thermodynamic factor was neglected.

Kinetics

The dimensionless reaction rate of the intercalation can be expressed by

$$\rho_j = \rho_{0,j} \cdot \left[\exp\left(\beta_{\mathrm{ox},j}\right) - \exp\left(-\beta_{\mathrm{red},j}\right)\right] \tag{14}$$

with the following definition of dimensionless exchange rate

$$\rho_{0,j} = \frac{j_{0,j}}{j_{0,j}^{\mathrm{ref}}} = f_{Li}^{\alpha_{\mathrm{ox},j}} \cdot \left(1 - f_{s,j}\right)^{\alpha_{\mathrm{ox},j}} \cdot f_{s,j}^{\alpha_{\mathrm{red},j}} \tag{15}$$

and corresponding overpotentials for oxidation and reduction.

$$\beta_j = b_j \cdot \eta_j \tag{16}$$

The reference exchange rate can be calculated using Equation (17):

$$j_{0,j}^{\mathrm{ref}} = k_j \cdot c_{\mathrm{Li},0}^{\alpha_{\mathrm{ox},j}} \cdot c_{s,\max,j}^{\alpha_{\mathrm{ox},j}+\alpha_{\mathrm{red},j}} \tag{17}$$

For galvanostatic operations, normalization of current density and cell voltage leads to Equations (18) and (19):

$$\mu = \mu_1 + \mu_2 = 1 \tag{18}$$

and

$$\nu = \varphi_1(\xi_c = 1) - \varphi_1(\xi_a = 0). \tag{19}$$

The general expression for dimensionless overpotentials reads

$$\frac{\eta_j}{U^{\mathrm{ref}}} = \varphi_1 - \varphi_2 - \nu_{0,j}. \tag{20}$$

Depending on the mode of operation, certain conventions have to be established. The reference time for galvanostatic operations can be defined as follows.

$$t^{\mathrm{ref}} = \frac{q_{\max}}{i} \tag{21}$$

However, the reference voltage for galvanostatic operations can be chosen arbitrarily. The preferred choice is the maximum value of the open-circuit voltage:

$$U^{\mathrm{ref}} = U_{0,c}(\mathrm{SoC}_c = 0) - U_{0,a}(\mathrm{SoC}_a = 1) \tag{22}$$

Another option according to Ref. [6] would be the definition

$$U^{\mathrm{ref}} = \frac{R \cdot T}{z \cdot F} \tag{23}$$

and using Equations (16) and (20), the dimensionless overpotential becomes

$$\beta_j = \alpha_j \cdot \left(\varphi_1 - \varphi_2 - \nu_{0,j}\right). \tag{24}$$

For potentiostatic operations, other conventions have to be defined. Clearly, the selected reference voltage should be the applied cell voltage, but for the current density a fixed value must be specified. Since the experiments were conducted at 1C, a corresponding reference time of 1 h was chosen.

Characteristic values

The dimensionless coefficients A_1–A_7 can be interpreted as characteristic values describing the performance of porous electrodes. The definitions and calculated values for both electrodes at galvanostatic operating mode are listed in Table 4. For the determination of all coefficients it was assumed that parameters are constant in the corresponding cell region.

The coefficient A_1 represents the ratio of diffusion time and operation time. Clearly, for low values of A_1, diffusion limits the performance of the battery. The dimensionless parameter A_4 has the same meaning for interstitial diffusion in the particles of the active material. In fluid mechanics and chemical reaction engineering there are similar characteristic values, for example the Péclet or Bodenstein numbers, which correlate the diffusion and dispersion with convection.

Table 4. Determination of characteristic values for LIB operation at 0.5C.

Definition	LIB test cell anode	cathode
$A_{1,j} = \frac{t^{\mathrm{ref}} \cdot D_{\mathrm{Li,eff}}}{\delta_j^2}$	561.4	175.9
$A_{2,j} = \frac{\varepsilon_{1,j} \cdot c_{s,\max,j}}{\varepsilon_j \cdot c_{\mathrm{Li},0}}$	15.5	21.1
$A_{3,j} = \frac{a_{v,j} \cdot j_{0,j}^{\mathrm{ref}} \cdot t^{\mathrm{ref}}}{\varepsilon_j \cdot c_{\mathrm{Li},0}}$	16.2	24.5
$A_{4,j} = \frac{t^{\mathrm{ref}} \cdot D_{s,j}}{R_{1,j}^2}$	~7.3	~17.4
$A_{5,j} = \frac{A_3}{A_2}$	1.04	1.16
$A_{6,j} = \frac{i \cdot \delta_j}{\sigma_{\mathrm{eff},j} \cdot U^{\mathrm{ref}}}$	$\sim 2.8 \cdot 10^{-6}$	$\sim 49.4 \cdot 10^{-6}$
$A_{7,j} = \frac{i \cdot \delta_j}{\kappa_{\mathrm{eff}} \cdot U^{\mathrm{ref}}}$	$2.3 \cdot 10^{-4}$	$6.0 \cdot 10^{-4}$

The second dimensionless coefficient A_2 can be simplified to

$$A_{2,j} = \frac{i \cdot t^{\mathrm{ref}}}{z \cdot F \cdot \delta_j \cdot \varepsilon_j \cdot c_{\mathrm{Li},0}} = \frac{\varepsilon_{1,j} \cdot c_{s,\max,j}}{\varepsilon_j \cdot c_{\mathrm{Li},0}}. \quad (25)$$

As one can easily see, this characteristic value is a measure for the ratio of the lithium reservoir in the active material and the lithium ion reservoir in the electrolyte. High values may indicate a lack of lithium salt in the solution.

The dimensionless parameter A_3 correlates the intercalation time with the operation time. In chemical reaction engineering, this characteristic value corresponds to the Damköhler number. For low values of A_3, the reaction is the limiting process for the battery performance.

Coefficient A_5 is the ratio of A_3 and A_2 [Eq. (26)]:

$$A_{5,j} = z \cdot F \cdot i^{-1} \cdot \delta_j \cdot a_{v,j} \cdot j_{0,j}^{\mathrm{ref}} = \frac{A_{3,j}}{A_{2,j}} \quad (26)$$

The last two coefficients, A_6 and A_7, can be identified as dimensionless resistances of electrodes and electrolyte, respectively. Thus, high values of these properties indicate increased voltage losses.

The dimensionless coefficients for the described LIB test cell at a current rate of 0.5C are presented in Table 4. Accordingly, a value of 1 h was chosen as the reference time t_{ref}. One can see that several characteristic values for anode and cathode have the same order of magnitude as exemplified by parameter A_2.

Significant differences are observed for the dimensionless resistances in the solid (A_6) and in the liquid phase (A_7) where the cathode exhibits much higher values. It is also noticeable that the impact of the electrolytic conduction is larger than that of the electrical conduction because the dimensionless resistances are higher. An important influence factor in both cases is the porosity of the corresponding electrode, which can be seen from the used correlations for effective values of the electrolytic and electrical conductivities given in Equations (29) and (31).

With respect to the diffusion-operation characteristics of electrolyte (A_1) and active material (A_4), it is found that the anode is more limited by the active material than the cathode whereas the cathode is more limited by the pore system than the anode. Overall, it can be stated that the limitation is caused by interstitial diffusion in both cases because of the low values for A_4. On the other hand, limitation due to reaction (A_3) is more significant for the anode. Taking the possible limitations by reaction and diffusion into account, one can state that the anode is the more limiting electrode even if the voltage losses are lower than for the cathode.

In this context, limitation does not mean that the charging or discharging process is limited in time but that the losses due to reaction and diffusion are dominating. As can be seen from Figure 4, the initially high anodic reaction overpotential

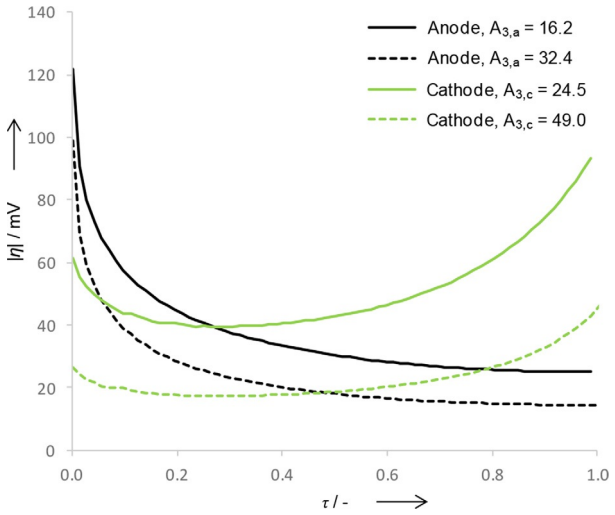

Figure 4. Average anodic and cathodic voltage losses due to reaction at 0.5C as a function of dimensionless charging time for two different values of the characteristic value A_3.

deteriorates rapidly and reaches nearly steady state after a certain time. On the other hand, the cathodic reaction overpotential is initially lower than for the anode, remains relatively unaltered with time, and finally increases strongly close to complete discharge. If now a doubling of the characteristic value A_3 for anode and cathode is assumed, the voltage losses due to reaction decrease in both cases as expected. The definition of A_3 given in Table 4 reveals that both the specific surface area of the electrode particles and the reference exchange rate could be increased for further reduction of the voltage losses. This example shows that the dimensionless value A_3 is a useful measure for the initial reaction limitation of a LIB electrode.

Conclusions

Characteristic values were worked out to evaluate a lithium-ion-battery (LIB) test cell and to compare the porous elec-

trodes used therein based on a chemical reaction engineering approach. For this purpose, conventions for galvanostatic and potentiostatic operation had to be defined because the newly developed dimensionless parameters depend on reference values for current density and cell voltage. Using the characteristic values, limiting processes can be detected. The evaluation of the electrodes showed that the cathode causes higher voltage losses, but the anode limits the performance of the full cell with regard to reaction and diffusion to a higher extent. The parameter analysis of a single characteristic value has validated the applicability of the analytical approach. Further parameter studies will be carried out to confirm these first results.

Experimental Section

The experimental data were measured using electrochemical test cells (ECC-Combi, EL-CELL GmbH, right side of Figure 5) em-

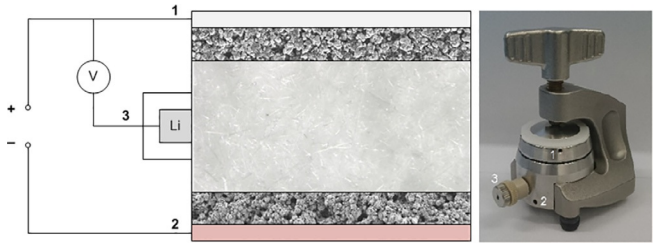

Figure 5. LIB test cell used; 1: working electrode; 2: counter electrode; 3: reference electrode.

ploying battery test systems BaSyTec CTS-LAB and Bio-Logic VSP. Glass fiber separators from Hollingsworth & Vose (nominal thickness 1.55 mm, porosity 92.2%, area density 27 mg cm^{-2}) were used due to the application of a lithium reference electrode, see left side of Figure 5. Parameters of the pressed separators were calculated according to manufacturer's specification. The electrolyte consisted of $LiPF_6$ in ethylene carbonate/diethylene carbonate (EC/DEC; mass ratio 3:7) denoted as LP47. The composition of the electrode layers produced at the Institute for Particle Technology (iPAT) at TU Braunschweig is presented in Table 5. Polyvinylidene fluoride (PVDF) was used as binder and carbon black (CB) was added for improving the conductivity.
The open-circuit potentials of the active materials were measured at twenty different states of charge and subsequently described using a ninth degree polynomial, see Equation (27). The results are shown in Figures 6 and 7.

$$U_0 = k_1 \cdot q^9 + k_2 \cdot q^8 + .. + k_9 \cdot q + k_{10} \quad (27)$$

The electrical conductivity of the electrodes was estimated by several measurements using dry electrodes. Coefficients of interstitial diffusion depend on the state of charge of the active mate-

Table 5. Composition of electrode layers.

Property	Fraction [%]					
	anode			cathode		
	SMG	PVDF	CB	LMO	PVDF	CB
mass	90	5	5	90	4	6
volume	88.2	6.1	5.7	80.2	8.3	11.5

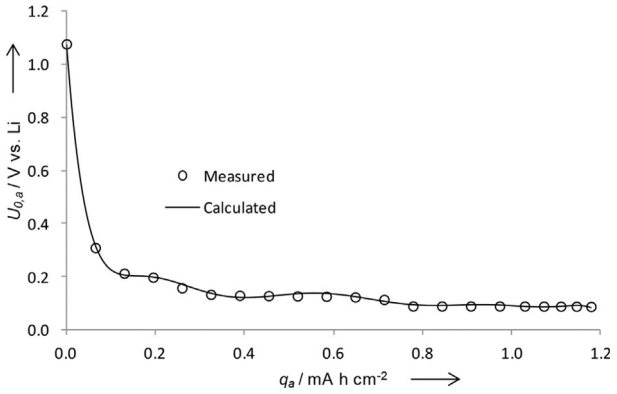

Figure 6. Open-circuit potential of the anode as a function of charge density.

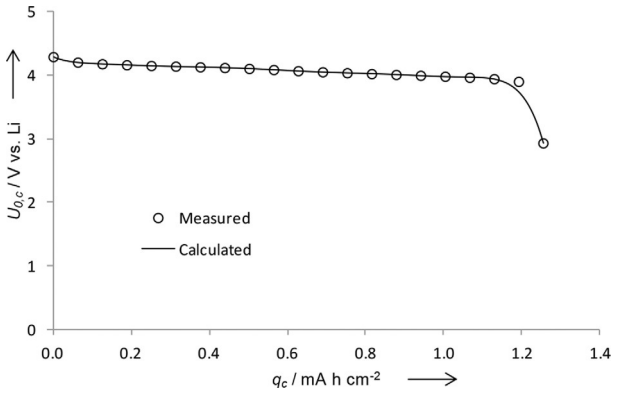

Figure 7. Open-circuit potential of the cathode as a function of charge density.

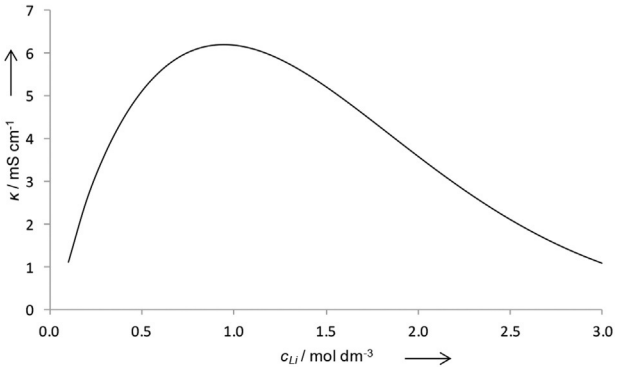

Figure 8. Electrolytic conductivity of LP47 according to Ref. [22].

rial,[19,20] thus average values were estimated.[21] The electrolytic conductivity depends on the lithium-ion concentration (Figure 8) and can be described with the Casteel–Amis equation [Eq. (28)].[22]

$$\kappa(c_{Li}) = \kappa_{max} \cdot \left(\frac{c_{Li}}{\mu}\right)^a \cdot \exp\left(b \cdot (c_{Li} - \mu)^2 - \frac{a}{\mu} \cdot (c_{Li} - \mu)\right) \quad (28)$$

Effective values of the transport properties were calculated using the corresponding porosities. The influence of tortuosity in the porous electrode structures can be considered by the Bruggeman correlation using an exponent of 1.5.[23,24]

$$\kappa_{\text{eff}} = \kappa \cdot \varepsilon^{1.5} \quad (29)$$

$$D_{\text{Li,eff}} = D_{\text{Li}} \cdot \varepsilon^{1.5} \quad (30)$$

$$\sigma_{\text{eff}} = \sigma \cdot (1 - \varepsilon) \quad (31)$$

The unit of reaction rate constant k (see Tables 1 and 6) depends on the values of the transfer coefficients:

$$X = 2 \cdot \alpha_{\text{ox}} + \alpha_{\text{red}} \quad (32)$$

Table 6. List of symbols.

Symbol	Description
A	area [m^2]
a_v	specific surface area [m^{-1}]
b	Tafel slope [V^{-1}]
c_{Li}	lithium ion concentration [$mol\,m^{-3}$]
c_s	lithium concentration [$mol\,m^{-3}$]
D_{Li}	lithium ion diffusion coefficient [$m^2\,s^{-1}$]
D_s	lithium diffusion coefficient [$m^2\,s^{-1}$]
F	Faraday constant ($F = 96485\ C\,mol^{-1}$)
i	current density [$A\,m^{-2}$]
j_0	exchange rate [$mol\,s^{-1}\,m^{-2}$]
j_p	reaction rate [$mol\,s^{-1}\,m^{-2}$]
k	reaction rate constant [$mol\,s^{-1}\,m^{-2}\,(m^3\,mol^{-1})^X$]
q	charge density [$A\,s\,m^{-2}$]
r	radial coordinate [m]
R	gas constant ($R = 8.314\ J\,mol^{-1}\,K^{-1}$)
R_1	average particle radius [m]
SoC	state of charge [%]
t	time coordinate [s]
t^0	transference number
T	temperature [K]
U	cell voltage [V]
U_0	open-circuit potential vs. Li [V]
x	spatial coordinate [m]
z	stoichiometric coefficient ($z = 1$)
α	transfer coefficient
δ	layer thickness [m]
ε	porosity [%]
ε_1	active material volume fraction [%]
η	overpotential [V]
κ	electrolytic conductivity [$S\,m^{-1}$]
σ	electric conductivity [$S\,m^{-1}$]
Φ	potential [V]
Subscript	
0	initial value
1	solid phase
2	liquid phase
a	anode
c	cathode
eff	effective value
j	cell region
Li	lithium ion
max	maximum value
ox	oxidation
red	reduction
ref	reference value

Acknowledgements

The authors would like to thank the Nds. Ministerium für Wissenschaft und Kultur of the State of Lower Saxony for the financial support of this work with Graduiertenkolleg Energiespeicher und Elektromobilität Niedersachsen (GEENI). We would like to thank all involved people at ICVT and EFZN for their kind support, especially Daniel Albrecht and Lei Shi, and we also gratefully acknowledge Christiane Schilcher from the iPAT at TU Braunschweig for providing the electrodes and helpful advice.

Keywords: batteries · chemical reaction engineering · dimensionless modeling · lithium · manganese

[1] J. O. Besenhard, G. Eichinger, *J. Electroanal. Chem.* **1976**, *68*, 1–18.
[2] G. Eichinger, J. O. Besenhard, *J. Electroanal. Chem.* **1976**, *72*, 1–31.
[3] J. B. Goodenough, Y. Kim, *Chem. Mater.* **2010**, *22*, 587–603.
[4] J. B. Goodenough, K.-S. Park, *J. Am. Chem. Soc.* **2013**, *135*, 1167–1176.
[5] V. Ramadesigan, P. W. C. Northrop, S. De, S. Santhanagopalan, R. D. Braatz, V. R. Subramanian, *J. Electrochem. Soc.* **2012**, *159*, R31–R45.
[6] S. Golmon, K. Maute, M. Dunn, *J. Power Sources* **2014**, *253*, 239–250.
[7] V. Srinivasan, J. Newman, *J. Electrochem. Soc.* **2004**, *151*, A1530–A1538.
[8] S. De, P. W. C. Northrop, V. Ramadesigan, V. R. Subramanian, *J. Power Sources* **2013**, *227*, 161–170.
[9] W. Du, N. Xue, A. Gupta, A. M. Sastry, J. R. R. A. Martins, W. Shyy, *Acta Mech. Sin.* **2013**, *29*, 335–347.
[10] R. E. Garcia, Y.-M. Chiang, W. C. Carter, P. Limthongkul, C. M. Bishop, *J. Electrochem. Soc.* **2005**, *152*, A255–A263.
[11] D. Zhang, B. N. Popov, R. E. White, *J. Electrochem. Soc.* **2000**, *147*, 831–838.
[12] M. Doyle, J. Newman, *Electrochim. Acta* **1995**, *40*, 2191–2196.
[13] Y. G. Chirkov, V. I. Rostokin, A. M. Skundin, *Russ. J. Electrochem.* **2011**, *47*, 1239–1249.
[14] W. Du, N. Xue, A. M. Sastry, J. R. R. A. Martins, W. Shyy, *J. Electrochem. Soc.* **2013**, *160*, A1187–A1193.
[15] T. F. Fuller, M. Doyle, J. Newman, *J. Electrochem. Soc.* **1994**, *141*, 1–10.
[16] S. Zugmann, M. Fleischmann, M. Amereller, R. M. Gschwind, H. D. Wiemhöfer, H. J. Gores, *Electrochim. Acta* **2011**, *56*, 3926–3933.
[17] J. Newman, K. E. Thomas-Alyea, *Electrochemical Systems, 3rd ed.*, Wiley, **2004**.
[18] S. Santhanagopalan, Q. Guo, P. Ramadass, R. E. White, *J. Power Sources* **2006**, *156*, 620–628.
[19] M. D. Levi, D. Aurbach, *Electrochim. Acta* **1999**, *45*, 167–185.
[20] P. P. Prosini, M. Lisi, D. Zane, M. Pasquali, *Solid State Ionics* **2002**, *148*, 45–51.
[21] Y. Ye, Y. Shi, N. Cai, J. Lee, X. He, *J. Power Sources* **2012**, *199*, 227–238.
[22] D. J. Moosbauer, *Ph. D. Thesis*, University of Regensburg, **2010**.
[23] I. V. Thorat, D. E. Stephenson, N. A. Zacharias, K. Zaghib, J. N. Harb, D. R. Wheeler, *J. Power Sources* **2009**, *188*, 592–600.
[24] D. A. G. Bruggeman, *Ann. Phys.* **1935**, *416*, 636–664.

Received: March 2, 2016
Revised: April 19, 2016
Published online on September 5, 2016

